Effects of 3-D Microwell Culture on Initial Fate Specification in Human Embryonic Stem Cells

Cheston Hsiao, Matthew Tomai, Jeremy Glynn, and Sean P. Palecek
Dept. of Chemical and Biological Engineering, University of Wisconsin-Madison, Madison, WI 53706

DOI 10.1002/aic.14351
Published online January 23, 2014 in Wiley Online Library (wileyonlinelibrary.com)

Several studies have demonstrated that three-dimensional (3-D) culture systems influence human embryonic stem cell (hESC) phenotypes and fate choices. However, the effect that these microenvironmental changes have on signaling pathways governing hESC behaviors is not well understood. Here, a 3-D microwell array was used to investigate differences in activation of developmental pathways between 2-D and 3-D cultures of both undifferentiated hESCs and hESCs undergoing initial differentiation in embryoid bodies (EBs). An increased induction into mesoderm and endoderm and differences in expression of genes from multiple signaling pathways that regulate development, including Wnt/β-catenin, TGF-β superfamily, Notch, and FGF during EB-mediated differentiation were observed in 3-D microwells as compared with the 2-D substrates. In undifferentiated hESCs, differences in epithelial-mesenchymal transition phenotypes and the TGFβ/BMP pathway between cultures in 3-D and 2-D were also observed. These results illustrate that 3-D culture influences multiple pathways that may regulate the differentiation trajectories of hESCs. © 2014 American Institute of Chemical Engineers *AIChE J*, 60: 1225–1235, 2014
Keywords: bioengineering, biomaterials, biomedical engineering

Introduction

Human embryonic stem cells (hESCs) have the potential to differentiate into over 200 diversely functioning cell types found in the human body.[1–3] The many processes involved in mammalian development, such as survival, self-renewal, and differentiation, are regulated by the microenvironment, which is the coordinated spatial and temporal presentation of molecular, structural, mechanical, and hydrodynamic cues.[4] To understand and control hESC behavior for downstream applications such as drug screening, tissue engineering, and regenerative medicine applications, *in vitro* studies that provide mechanistic understanding of how the physiologically relevant three-dimensional (3-D) microenvironment regulates hESC fates will be necessary.

To this end, various materials-based culture platforms have been engineered to systematically study how microenvironmental contributions, such as substrate stiffness, extracellular matrix (ECM) proteins, scaffolding, and mechanical stimuli, affect ESC behavior.[5–10] 3-D microwell cell culture platforms have been utilized to modulate cell–cell contact, intercellular, and autoregulatory signaling that occur in hESCs and during differentiation, particularly in embryoid body (EB)-based differentiation.[11] Some studies have demonstrated that pro-pluripotency autoregulation can be accentuated in various configurations of 3-D microwell culture.[12–14] In addition, many studies have demonstrated that microwell culture affects differentiation toward multiple cell types including hematopoietic lineages,[15] myeloid and erythroid cells,[16] and cardiomyocytes.[17–19]

However, very little is yet known regarding the molecular mechanisms by which 3-D microwell culture drive the significant differences in cell fate observed. A study by Azarin et al.[20] showed that hESCs cultured in microwells exhibited less nuclear β-catenin when compared to hESCs cultured on 2-D substrates. However, upon enzymatic removal of hESC colonies from microwells and EB differentiation, significantly higher canonical Wnt signaling was observed in EBs made from microwell-cultured hESCs. The cells that demonstrated higher levels of Wnt signaling activity exhibited greater expression of genes associated with the primitive streak, mesoderm, and cardiac lineage. In another study by Hwang et al.,[21] EBs derived from murine ESCs cultured in microwell sizes that favored cardiogenesis over endothelial cell differentiation expressed noncanonical Wnt11 at a greater level than Wnt5a. Upon siRNA knock down of Wnt5a, endothelial vessel sprouting was ablated while cardiac markers became highly expressed. Exogenous Wnt5a addition increased the expression of endothelial markers and the sprouting of endothelial vessel structures, though with no significant change to cardiac markers. Finally, a study by Bauwens et al.[22] described a cellular mechanism by which microwell-derived EBs of different sizes influenced differentiation potential. They posited that EB size specified the outer surface area-to-volume ratio, which determined the amount of cardiac-promoting extraembryonic endoderm cells

Additional Supporting Information may be found in the online version of this article.

Correspondence concerning this article should be addressed to S. P. Palecek at palecek@engr.wisc.edu.

in the EB, thus promoting cardiomyogenesis. Much has yet to be identified regarding the milieu of molecular mechanisms by which morphology of ESC colonies regulates developmental signaling pathways and affects lineage commitment.

Therefore, using a microwell system previously established in our lab,[13] we sought to identify major signaling pathways modulated by 3-D microwell culture of hESCs in the undifferentiated state and also during subsequent EB differentiation. In undifferentiated hESCs cultured in 3-D vs. 2-D, we observed differences in epithelial-mesenchymal transition (EMT) and the TGFβ/BMP pathway. However, comparing 3-D EB-mediated differentiation of aggregated hESCs cultured from 3-D microwells vs. 2-D substrates, we observed increased induction into mesoderm and endoderm, and differences in expression of genes from multiple signaling pathways that regulate development, including Wnt/β-catenin, TGF-β superfamily, Notch, and FGF.

Materials and Methods

Microwell fabrication

Microwells were prepared in three major steps as previously described.[13] First, silicon master molds with desired microwell patterns were made using hard lithography techniques. The cuboidal microwells had lateral dimensions of 300 μm and a depth of 120 μm. These master molds were fluorinated with (tridecafluoro-1,1,2,2,-tetrahydrooctyl)-1-trichlorosilane vapor to passivate the surface and minimize fouling. Second, via soft-lithography, polydimethylsiloxane (PDMS) stamps were formed with the inverted pattern from the silicon masters. Finally, these PDMS stamps were elevated over glass microscope slides with 250 μm spacers. In the space between, polyurethane prepolymer was fed, distributed via capillary action and crosslinked under UV light yielding patterned microwells.

Preparation of microwells for cell seeding

On the areas surrounding the wells, microwells were coated with an 80 Å titanium layer followed by a 200 Å gold layer via e-beam evaporation. After sterilization with UV and 100% ethanol, microwell slides were immersed in tri(ethylene glycol)-terminated (EG3) alkanethiol self-assembling monolayer (SAM) solution overnight. This SAM functionalized only on the surfaces coated with gold while the EG3 functional group prevented protein adsorption and subsequent cell attachment. Thus, of the approximate 250 mm^2 total surface area of the microwell array, about 45 mm^2 are available for protein adsorption. After washing in ethanol, functionalized microwells were coated with growth factor reduced Matrigel for at least 1 h at 37°C. To seed the microwells, cells were singularized via Accutase (Innovative Cell Technologies), resuspended in CM/F+ at 1×10^6 cells/100 μL/microwell slide, and aliquoted to the top of each microwell array. The cell solution was maintained on top of arrays for at least 15 min to allow cells to settle into microwells before adding 2 mL/well of CM/F+. A flowchart of microwell fabrication and cell seeding is represented in Figure 1.

hESC culture and embryoid body differentiation

H9 hESCs were cultured on tissue culture polystyrene (TCPS) coated with growth factor reduced Matrigel (BD Bioscience) for at least 1 h at 37°C. Unconditioned medium (UM/F−) composed of DMEM/F12 culture medium (Invitrogen) containing 20% KnockOut Serum Replacer (Invitrogen), 0.1 mM MEM nonessential amino acids (Invitrogen), 1 mM L-glutamine (Invitrogen), and 0.1 mM β-mercaptoethanol (Sigma) was conditioned on irradiated mouse embryonic fibroblasts for 24 h and supplemented with 4 ng/mL bFGF (Invitrogen), which resulted in the culture medium CM/F+.

For EB differentiation studies, hESCs were cultured on TCPS or in microwells for 6 days in CM/F+. To initiate differentiation, colonies were detached from the Matrigel matrix at day 6 of culture using 1 mg/mL dispase (Invitrogen) and placed in suspension in UM/F− in Corning 3741 ultralow attachment plates. Following 24 h in UM/F−, the EBs were maintained in suspension for 4 more days in EB20 medium: DMEM/F12 containing 20% fetal bovine serum (Invitrogen), 0.1 mM nonessential amino acids, 1 mM L-glutamine, and 0.1 mM β-mercaptoethanol.

RT-PCR and quantitative RT-PCR

For RNA extraction, cells were dissociated with Versene (Invitrogen), Accutase (Innovative Cell Technologies), TrypLE (Invitrogen), or 0.25% Trypsin-EDTA (Invitrogen). Total RNA was extracted using an RNeasy MiniKit (Qiagen) according to the manufacturer's instructions and treated with DNase I (Invitrogen). cDNA was generated from 1 μg of RNA using Omniscript reverse transcriptase (Qiagen) and Oligo-dT(20) primers (Invitrogen). End-point PCR was performed with GoTaq Green Master Mix (Promega) and then subjected to 2% agarose gel electrophoresis and imaged using ethidium bromide. Amplicon band intensity was semiquantified using ImageJ with *GAPDH* and *ACTB* used as endogenous controls. Quantitative RT-PCR (qPCR) was performed using iQ SYBR Green Supermix (Bio-Rad) on an iCycler (Bio-Rad).

Western blot analysis

Cells were lysed in mammalian protein extraction reagent (Pierce) in the presence of halt protease and phosphatase inhibitor cocktail (Pierce). Proteins were separated by 10% Tris-Glycine SDS-PAGE under denaturing conditions and transferred to a nitrocellulose membrane. After blocking with 5% BSA or Milk in TBS + 0.1% Tween-20, the membrane was labeled with primary antibody overnight at 4°C. The membrane was then washed and incubated with a horseradish peroxidase-conjugated secondary antibody for 1 h at room temperature or overnight at 4°C. Protein levels were detected via a SuperSignal West Pico Chemiluminescent Substrate (Pierce). Equal protein loading was confirmed via β-actin and GAPDH levels. Band intensity was quantified using Image Lab Software (BIO-RAD).

Flow cytometry

Cells were dissociated into single cells and then fixed with 1% paraformaldehyde for >20 min at room temperature and permeabilized in ice-cold 90% methanol for at least 30 min. Primary antibodies were incubated overnight in PBS plus 0.1% Triton X-100 and 0.5% BSA. Data were collected on a FACS Caliber flow cytometer (Beckton Dickinson) and analyzed using FlowJo.

Statistics

Data are presented as mean ± standard deviation (SD) and *P*-values were determined using an unpaired Student's *t*-test.

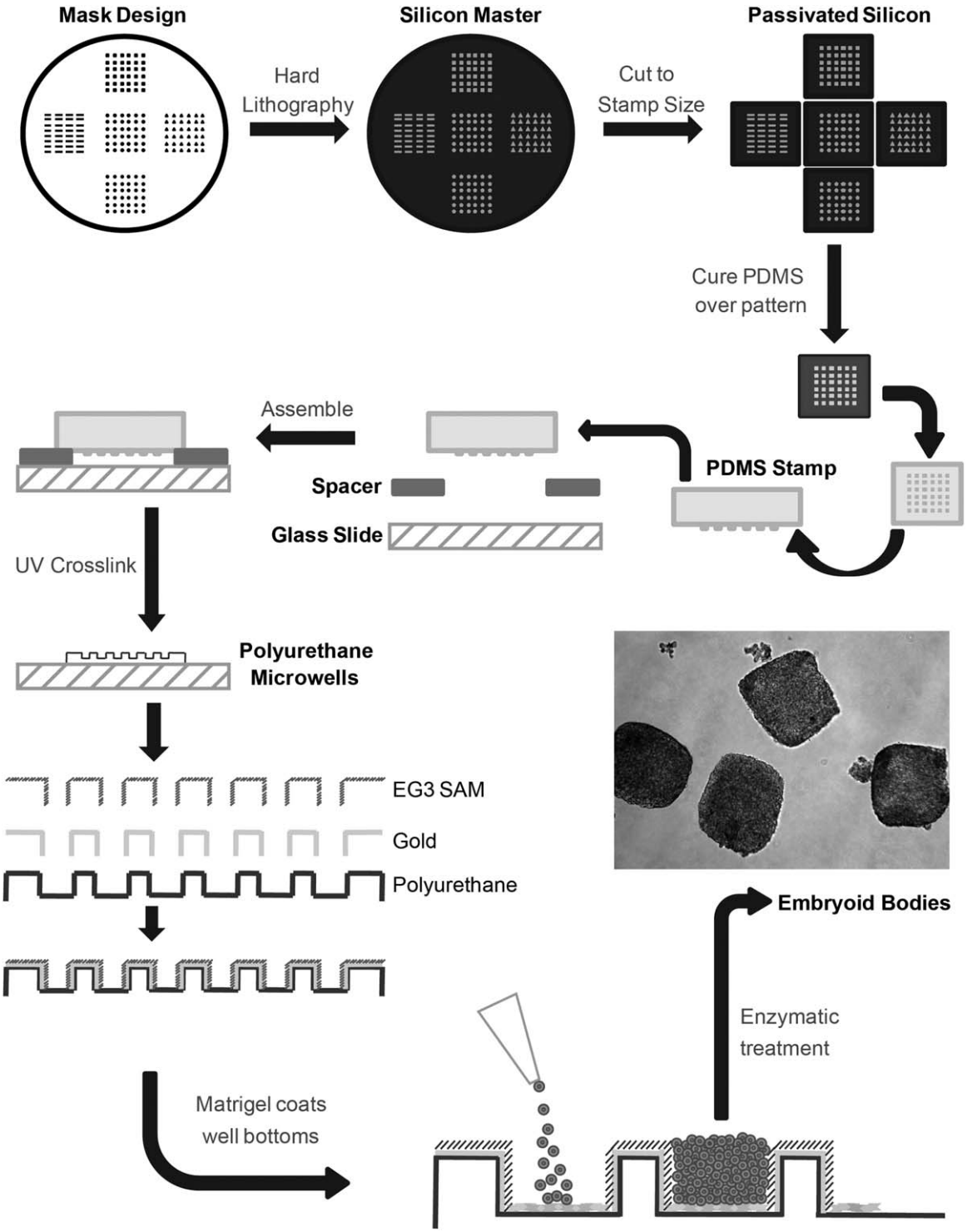

Figure 1. Schematic of 3-D microwell design, manufacturing, and preparation for cell culture.

Silicon master molds were fabricated via hard lithography. The master molds were passivated to pattern PDMS stamps. The reusable stamps were then elevated over glass slides with spacers. Polyurethane prepolymer filled the space and was UV-crosslinked to form polyurethane microwells. E-beam evaporation was then used to coat the areas outside of the wells with a thin layer of gold. Finally, a tri(ethylene glycol)-terminated alkanethiol self-assembled monolayer (EG3) was assembled on the gold surface. This confers protein resistance on all but the bottom of the microwells. Cells were seeded into the microwells and allowed to grow for 6 days before enzymatic detachment and EB formation to initiate differentiation. The phase contrast inset shows suspended cell aggregates immediately after microwell colonies were detached.

Results

Microwell culture increased induction into mesendoderm in embryoid bodies

As previously demonstrated,[18] the differentiation of hESCs into cardiomyocytes can be enhanced by culturing the hESCs in 3-D microwell systems prior to inducing differentiation in EBs. Differentiation to functional, contracting cardiomyocytes did not occur until at least 9 days after hESC colony removal from microwell culture. However, as the direct effects from microwell culture end upon EB formation, we

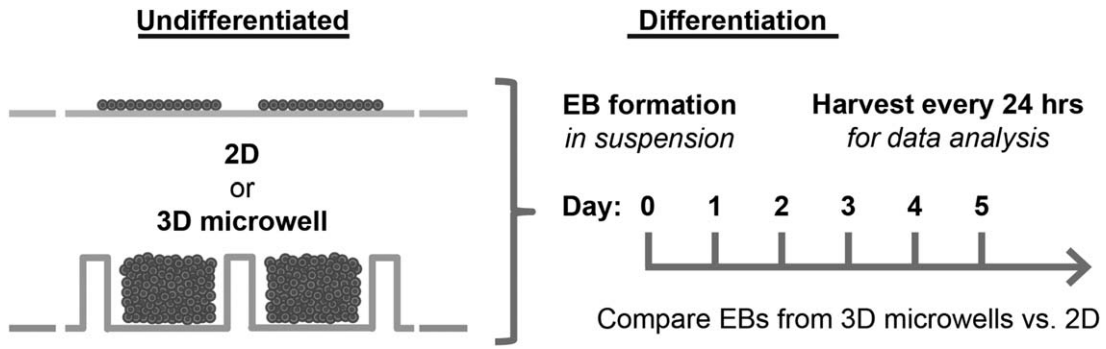

Figure 2. Schematic representation of the experimental plan.

Undifferentiated hESCs were cultured either on 2-D TCPS or in 3-D microwells. After 6 days in culture as undifferentiated cells, colonies were enzymatically detached and placed in suspension to initiate EB formation and differentiation. EBs were collected immediately after removal from the substrate and every 24 h following for data analysis to compare differences between EBs generated from 2-D and 3-D microwell culture of undifferentiated hESCs.

expect to observe differences in differentiation trajectory at much earlier developmental stages, including exit from pluripotency and germ lineage specification. The earliest steps in cardiogenesis involve the induction of pluripotent hESCs into mesendoderm and precardiac mesoderm, which are specified during gastrulation *in vivo*.

To ascertain whether microwell culture influences induction into mesendoderm during early EB differentiation, hESCs were seeded into Matrigel-coated 3-D microwells. The protein-resistant SAM prevented cell attachment on all but the bottom of the microwells. hESCs were also seeded onto Matrigel-coated TCPS as a control representing traditional 2-D culture of ESCs. After 6 days of culture in CM/F+, hESCs were enzymatically removed and cultured in suspension to form EBs. Cells were harvested for PCR, flow cytometry, and/or western blot analysis immediately prior to suspension culture and after selected number of days in suspension culture. A schematic representation of the general experimental plan is shown in Figure 2.

The expression of *POU5F1* (Oct4) decreased at similar rates in EBs made from hESCs cultured on 2-D TCPS and in 3-D microwells, though the EBs from microwell-cultured hESCs continued to express more *POU5F1* through day 4 of EB formation (Figure 3A). The percentage of Oct4 positive cells was nearly zero by the seventh day of EB formation from both 2-D TCPS and 3-D microwell culture, though EBs from microwell-cultured hESCs exhibited a higher percent of Oct4 positive cells at day 4 of EB formation (Figure 3B).

We observed significant differences in expression of the transcription factors that control induction into the germ layers associated with cardiogenesis. The expression of *SOX17,* a marker of embryonic definitive endoderm, was detected by the third day of formation of EBs from microwell-cultured hESCs, which was about a day before detection of *SOX17* in EBs made from 2-D cultured hESCs. *SOX17* expression continued to rise through the fourth day of EB differentiation (Figure 3C). This correlated with a higher percentage of cells expressing Sox17 protein in the EBs from microwell-cultured hESCs as compared to EBs made from 2-D culture (Figure 3D). Importantly, there was a strong peak in expression of *T* gene (Brachyury), which encodes a transcription factor that controls mesendoderm induction early after loss of pluripotency,[23] at days 3 and 4 in EBs made from microwell-cultured hESCs, but no such peak in *T* expression in EBs made from hESCs cultured on 2-D TCPS (Figure 3E). A similar peak at days 3 and 4 was observed in the expression of additional mesendoderm markers *GSC*[24] and *MIXL1*[25] (Figure 4). A corresponding peak in the expression of Brachyury protein was also observed at day 3 (Figure 3F). This profile suggests EBs from hESC-cultured microwells favor mesendoderm lineages.

Though the enhancement in definitive cardiomyocyte specification from microwell culture was not observed until 1.5 weeks after the start of EB differentiation via functional beating or flow cytometry for cardiomyocyte markers,[18] the earliest markers of mesendoderm specification, an event in cardiac development, were observed as early as 3 days after EB formation. Thus, microwell culture influences the differentiation trajectory that correlates with the differences in cardiomyocyte differentiation observed at later times.

Differences in gene expression of multiple signaling pathways in EBs from microwell and 2-D culture

To broaden our understanding of the potential differences that occur during the differentiation of EBs made from hESCs grown in 3-D microwells or on 2-D TCPS, expression of genes related to signaling pathways and cellular transitions involved in hESC differentiation was surveyed. These include the Wnt/β-catenin pathway, TGF-β superfamily, Notch pathway, FGF signaling, and EMT. Though this analysis was not comprehensive, it illustrated major differences in signaling pathway gene expression in hESCs cultured in 2-D and 3-D when subjected to differentiation in EBs.

To identify differences in gene expression in EBs, hESCs were seeded into Matrigel-coated microwells or on 2-D plates as previously described. After 6 days of expansion, hESCs were enzymatically removed and cultured in suspension to form EBs. Cells were harvested for RNA purification and RT-PCR immediately prior to suspension culture and every day for 5 days. The amplified products were run on an agarose gel and the intensities were quantified to the intensities of housekeeping genes *GAPDH* and *ACTB*. Finally, the quantified intensities of each gene were standardized in Matlab across each of the biological samples and are presented as a heatmap (Figure 4), with the values provided in Supplementary Table 1.

As expected, there was a strong upregulation of genes associated with the mesendoderm lineage and early cardiogenesis, including *ISL1*, *GATA4*, and *NKX2–5*, at day 3 of differentiation in EBs formed from microwell-cultured

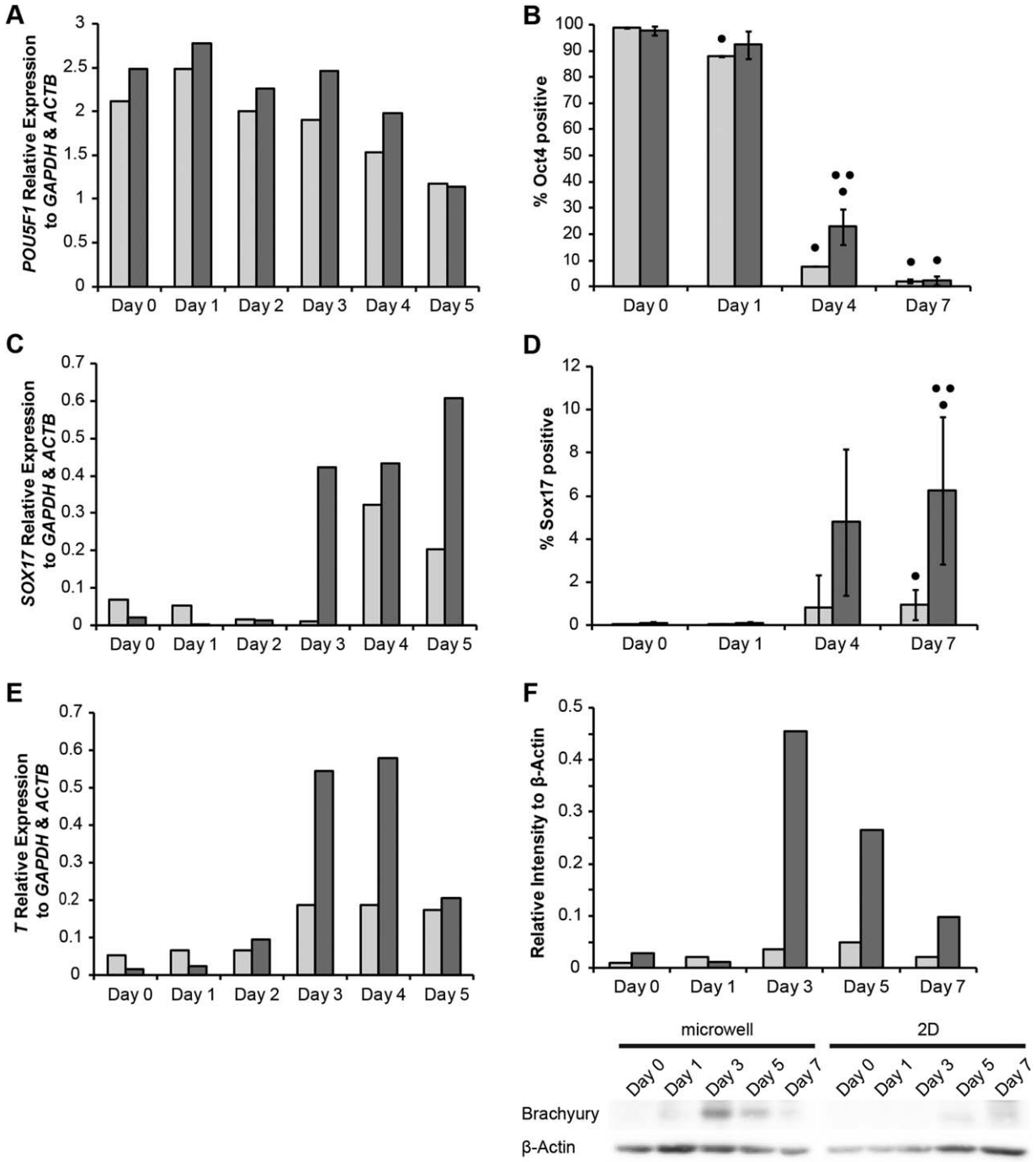

Figure 3. Comparison of early differentiation trajectory of 2-D TCPS-cultured hPSCs and 3-D microwell-cultured hPSCs.

(A) RT-PCR quantification of *POU5F1* expression in EBs 0–5 days after formation from hESCs cultured on Matrigel-coated TCPS (2-D, light) and 3-D microwells (dark) relative to expression of *GAPDH* and *ACTB*.

(B) Flow cytometry for percentage Oct4-positive cells of EBs days 0, 1, 4, and 7 after formation. (C) RT-PCR quantification of *SOX17* expression, relative to expression of *GAPDH* and *ACTB*, in EBs 0–5 days after formation from hESCs cultured on either 2-D TCPS or in 3-D microwells. (D) Flow cytometry for percentage Sox17-positive cells in EBs days 0, 1, 4, and 7 after formation. (E) RT-PCR quantification of *T* expression in EBs days 0–5 after formation from hESCs cultured on either 2-D TCPS or in 3-D microwells. (F) A representative western blot of Brachyury in EBs from hESCs cultured from either 2-D TCPS or 3-D microwells is shown with quantification of western blot intensities of Brachyury relative to housekeeping β-actin. (• indicates $P < 0.05$ compared to day 0, •• indicates $P < 0.05$ compared to same-day 2-D control).

hESCs. Moreover, there was also an upregulation of the genes responsive to Wnt signaling, such as *WNT3A*, *WNT8A*, and *LEF1*, at day 3 of differentiation in EBs formed from microwell-cultured hESCs. These two trends had very similar expression profiles. Interestingly, some target genes of Wnt signaling, including *DKK1* and *BCL9*, were upregulated in EBs from microwell-cultured hESCs even before the third day of differentiation.

Genes associated with the Notch pathway, FGF pathway, and TGF-β superfamily were also generally upregulated in

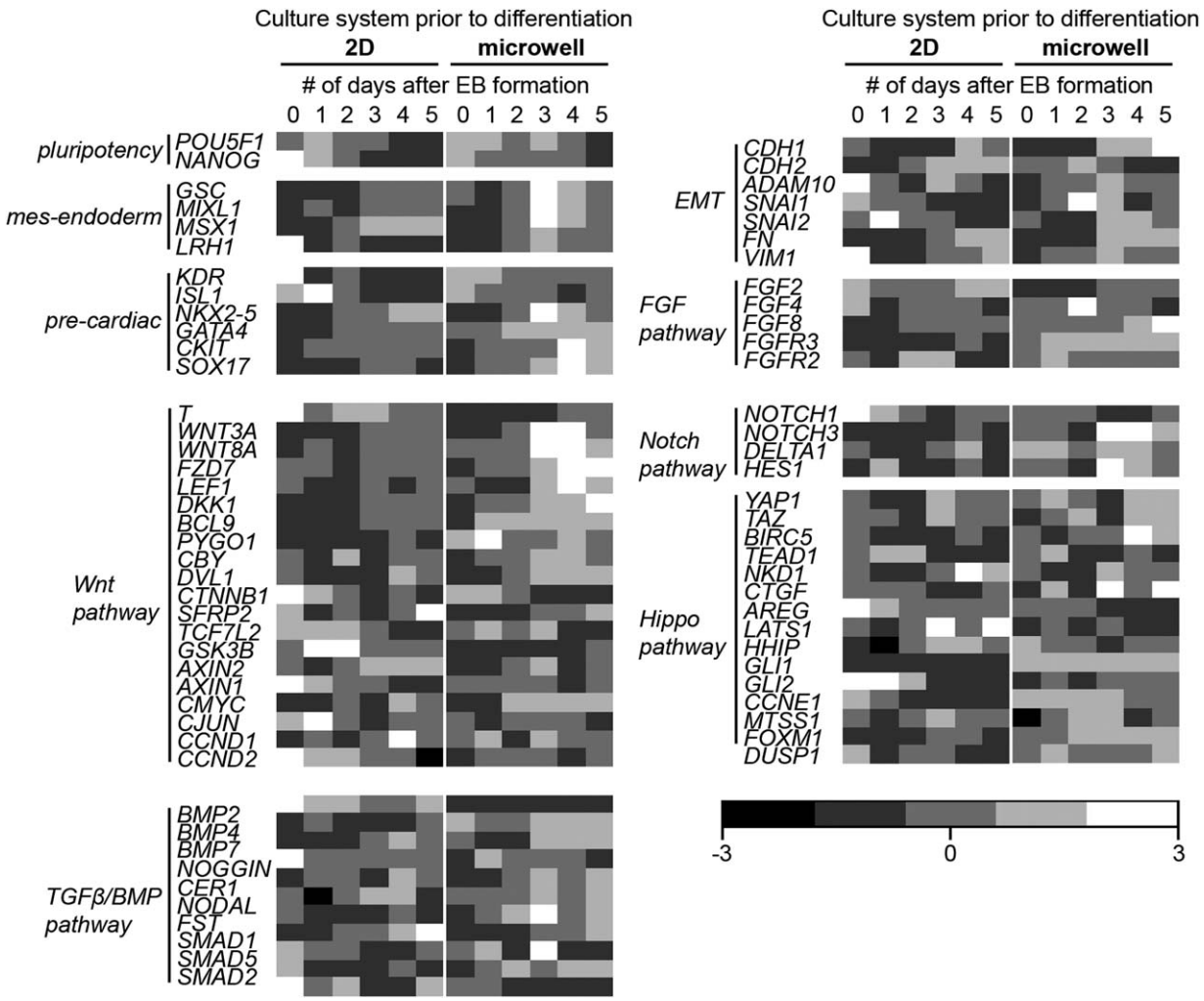

Figure 4. Gene expression heat maps in EBs from 2-D TCPS-cultured hESCs and 3-D microwell-cultured hESCs.

RT-PCR quantification of gene expression, normalized to *GAPDH* and *ACTB*, in EBs 0–5 days after formation from hESCs cultured on 2-D TCPS or in 3-D microwells. RT-PCR analysis of pluripotent, mesendoderm, precardiac, FGF pathway, Wnt pathway, Notch pathway, Hippo pathway, and TGFβ/BMP pathway was performed. Values along each row (representing a single gene) were normalized so that the mean equals 0 and the SD equals 1. Lighter shades of gray indicate higher (>0) expression and darker shades of gray indicate lower (<0) expression.

EBs derived from microwell-cultured hESCs. Genes in the Notch pathway such as *NOTCH1* and *DELTA1* were upregulated in EBs made from microwell-cultured hESCs by day 3 of differentiation, whereas *NOTCH3* was upregulated throughout differentiation. Similarly, *FGF2* and *FGF8*, genes in the FGF pathway, were upregulated in EBs from microwell-cultured hESCs by the first day of differentiation. Representative genes from the TGF-β superfamily, such as *BMP2*, *BMP7*, *NOGGIN,* and *NODAL*, were also upregulated in EBs from microwell-cultured hESCs when compared to those from TCPS-cultured hESCs.

Differences in EMT phenotypes and TGFβ/BMP pathway activation in hESCs in 3-D and 2-D culture

While a general upregulation of Wnt, FGF, TGFβ, and Notch family genes was observed during EB-based differentiation of hESCs cultured in microwells, there was also modular expression of some developmentally important signaling pathway genes between undifferentiated hESCs cultured in 3-D microwells or on 2-D TCPS. Such differences included genes related to epithelial and mesenchymal phenotypes and members of the TGFβ/BMP signaling pathway. Thus, differences in gene expression were supplemented with analysis of protein expression and activation.

To study differences in phenotypes of undifferentiated hESCs, cells were seeded into Matrigel-coated 3-D microwells or 2-D TCPS substrates. After 3 or 6 days of culture in CM/F+, hESCs were harvested for PCR, flow cytometry, and/or western blot analysis.

First, cells cultured in microwells exhibited reduced expression of markers associated with mesenchymal-like cells and the EMT, such as *FN* and *CDH2* (Figure 5A). Conversely, a marker of epithelial-like cells, *CDH1*, was slightly upregulated. This trend suggests that the cells cultured in microwells exhibit a more epithelial phenotype, possibly due to increased cell–cell contact from neighboring cells in 3-D culture. *CDH1* encodes for E-cadherin, the protein necessary for the establishment and maintenance of cell–cell contact in adherens junctions. Thus, by measuring the amount of E-cadherin per cell, the degree of functional cell–cell contact per cell can also be determined. Therefore, the intensity of E-cadherin expression per cell was quantified using flow cytometry. The average fluorescence intensity of E-cadherin per cell was $\sim$50% greater

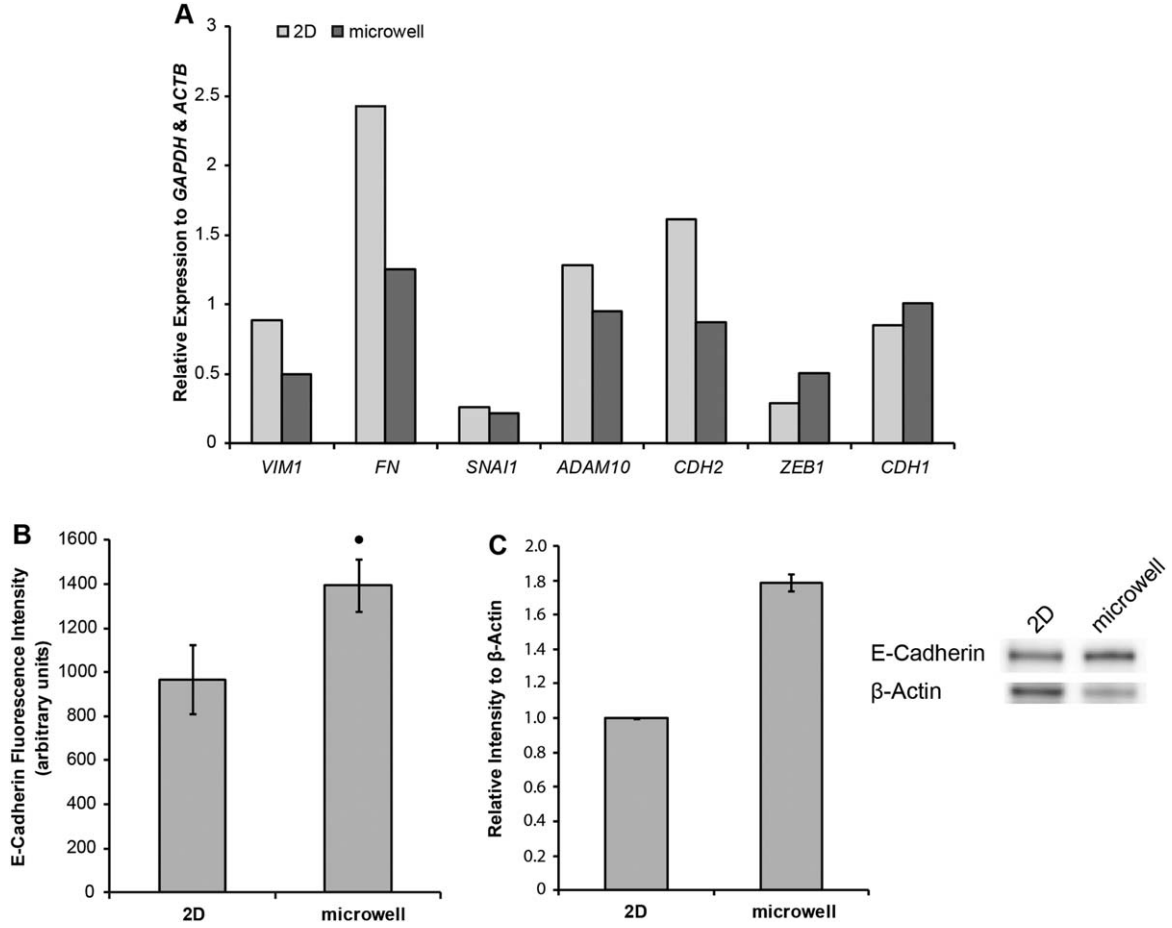

Figure 5. Epithelial-mesenchymal transition in hESCs cultured on 2-D TCPS and in 3-D microwells.

(A) Quantification of representative EMT-related gene expression agarose gel bands, relative to *GAPDH* and *ACTB*, in undifferentiated hESCs cultured for 6 days on 2-D TCPS (light) and in 3-D microwells (dark).

(B) Average intensity of E-cadherin fluorescence per cell, determined by flow cytometry, in undifferentiated hESCs cultured on 2-D TCPS and in 3-D microwells. (C) Quantification of western blot intensities of E-cadherin relative to β-actin in biological replicates of hESCs cultured for 6 days on 2-D TCPS or in 3-D microwells. Sample western blots representative of data are shown (• indicates $P < 0.05$ compared to same-day 2-D control).

in cells cultured in 3-D microwells than cells cultured on 2-D TCPS (Figure 5B). The elevated expression of E-cadherin in hESCs cultured in microwells vs. TCPS was confirmed via western blot analysis (Figure 5C).

Another developmental signaling pathway regulated by microwell culture is the TGF-β superfamily. While the TGF-β superfamily interactome is extensive, most signaling channels through the Smad family of intracellular transcriptional mediators. In the Smad family, receptor-regulated Smads (R-Smads) are phosphorylated by receptor kinases that respond to specific TGF-β superfamily ligands.[26] For example, Smad2 and Smad3 are phosphorylated by TGFβ/Activin/Nodal receptors, and Smad1, Smad5, and Smad8 are phosphorylated by BMP receptors. Once phosphorylated, these R-Smads complex with a single co-Smad, Smad4, and translocate into the nucleus to regulate gene expression. Thus, R-Smad phosphorylation can serve as an indicator of TGFβ/Activin/Nodal or BMP signaling.

NODAL and *GDF11*, genes related to TGFβ/Activin/Nodal signaling, exhibited reduced expression in hESCs in microwells as compared hESCs on TCPS (Figure 6A). To determine whether the downregulation in expression of these genes correlated with less Smad2 signaling, the protein level of phosphorylated Smad2 was measured via western blot. The relative protein level of phosphorylated Smad2 to β-actin was found to be lower in hESCs cultured in microwells as compared to those on a 2-D substrate (Figure 6B). Together, the gene expression and phosphorylated Smad2/3 levels suggest that the cells cultured in 3-D microwells compared to 2-D surfaces may transduce less signaling through the TGFβ/Activin/Nodal pathway.

The expression of genes associated with the BMP branch of the TGF-β superfamily did not provide clear evidence of activation or repression in 3-D vs. 2-D culture (Figure 6C). In hESCs cultured in microwells, there was greater expression of some BMP ligands, such as *BMP2* and *BMP4* and less expression of other BMP ligands, such as *BMP7*. The expression of the BMP ligand inhibitor *NOGGIN* was upregulated in microwells, but expression of the inhibitor *CHRD1* was diminished. However, the cells in microwells exhibited a greater ratio of phosphorylated Smad 1/5 than those in 2-D culture (Figure 6D), suggesting elevated BMP associated Smad signal transduction in 3-D compared to 2-D.

Discussion

In this study, we utilized a microwell system to observe how major signaling pathways in hESCs are affected by

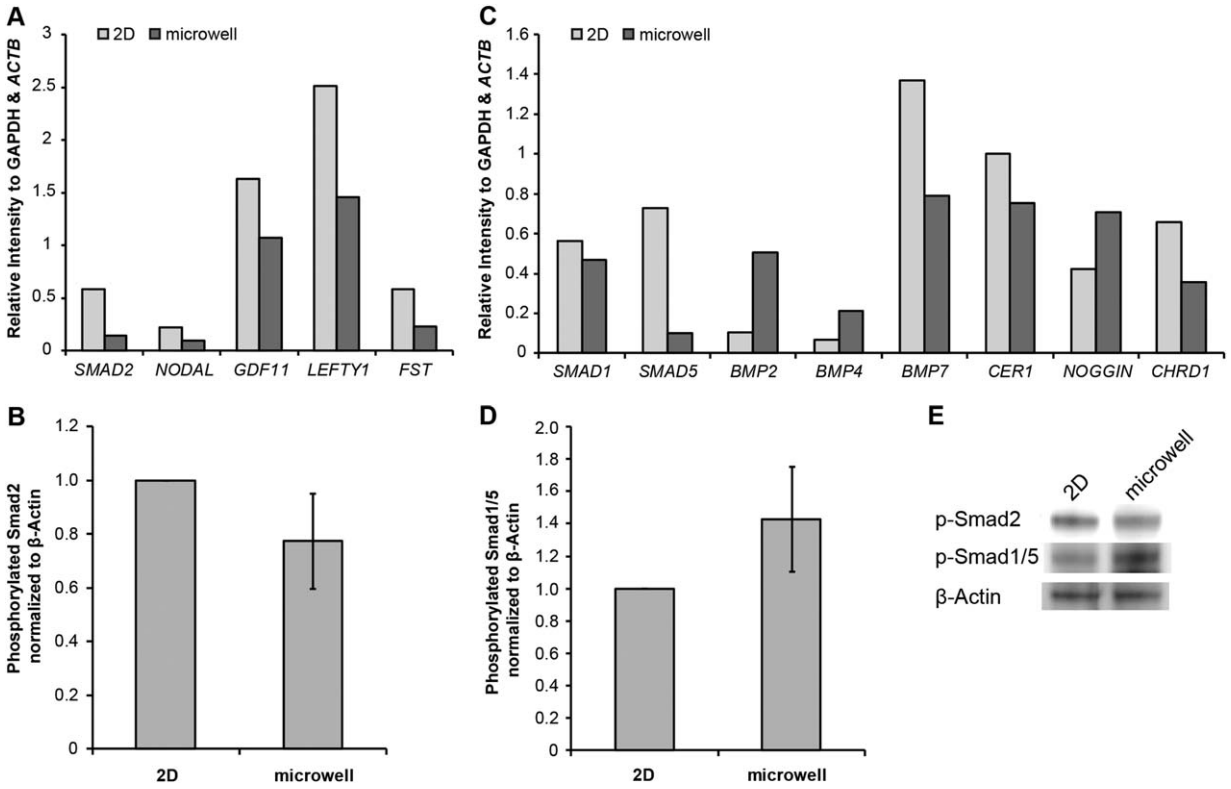

Figure 6. TGFβ superfamily signaling in hESCs cultured on 2-D TCPS and in 3-D microwells.

(A) Quantification of representative TGFβ/Activin/Nodal pathway gene expression agarose gel bands, normalized to *GAPDH* and *ACTB* expression in undifferentiated hESCs cultured for 6 days on 2-D TCPS (light) or in 3-D microwells (dark).

(B) Quantification of western blot intensities of phosphorylated Smad2 normalized to β-actin in biological triplicates of protein extracts obtained from undifferentiated hESCs cultured for 6 days on 2-D TCPS or in 3-D microwells. Quantification of intensities was normalized to 2-D samples. (C) Quantification of representative BMP pathway gene expression agarose gel bands, relative to *GAPDH* and *ACTB,* in undifferentiated hESCs cultured for 6 days on 2-D TCPS (light) and in 3-D microwells (dark). (D) Quantification of western blot intensities of phosphorylated Smad1/5 normalized to β-actin in biological triplicates of protein extracts obtained from undifferentiated hESCs cultured for 6 days on 2-D TCPS or in 3-D microwells. Quantification of intensities was normalized to 2-D samples. (E) Sample western blots representative of data in panels (B) and (D).

culturing within a 3-D microenvironment while in the undifferentiated state and also during subsequent EB differentiation. Based upon previous work,[18,20] we hypothesized that the gene targets of the canonical Wnt signaling pathway would be upregulated in the EBs made from microwells. Moreover, we hypothesized that many of the markers for the earliest stages of cardiogenesis would also be upregulated in the EBs made from microwells. Not only did we see an upregulation of multiple direct gene targets of canonical Wnt signaling, we also observed a corresponding upregulation in mesendoderm genes (*T*, *GSC*, *MIXL1*, and *SOX17*) and early cardiac mesoderm genes (*ISL1* and *NKX2–5*). Moreover, we observed a higher percentage of Brachyury and Sox17-expressing cells in EBs formed from microwells. Sox17, an endodermal transcription factor, has been shown to be indispensable for cardiac myogenesis.[27] The *T* gene that encodes Brachyury is a direct gene target of Wnt signaling in ESCs.[28] Furthermore, our group has also demonstrated that by modulating the Wnt signaling pathway alone, a high yield and purity of cardiomyocytes can be generated from ESCs.[29,30] Thus, information garnered from the study of the effects from 3-D culture is pertinent to understanding the signaling pathways important during cardiogenesis.

Several studies have demonstrated that the proper balance and timing of TGFβ/Activin/Nodal and BMP signaling can induce cardiogenesis in hESCs *in vitro*.[31–34] Moreover, these pathways are known to regulate gastrulation, primitive streak formation, and mesendoderm specification.[35] Accordingly, our gene expression data demonstrate that TGFβ signaling pathways are influenced by 3-D culture prior the start of differentiation and upregulated during EB differentiation of microwell-cultured hESCs. Activin/Nodal and BMP signaling is induced by activating Wnt pathway via GSK3β-inhibitors during directed cardiomyocyte differentiation.[29] However, during EB-based differentiation from microwell-cultured hESCs, it is unclear how the interplay and crosstalk between these developmental signaling pathways operates. Also of note, immediately after differentiation began, we noticed an upregulation in FGF-related genes such as *FGF4* and *FGF8*. *FGF4* synergizes with BMP signaling to induce cardiogenesis[36] and both *FGF4* and *8* are known to be essential during primitive streak establishment and mesoderm formation.[37]

Interestingly, genes associated with the Notch pathway were upregulated in EBs made from microwell-cultured hESCs compared to TCPS-cultured hESCs. In prior ESC differentiation studies, activation of the Notch pathway during early differentiation was associated with neural commitment[38,39] and is not believed to directly specify cardiac mesoderm during early stages of mesoderm formation in the primitive streak.[40] However, the context of Notch signaling

may direct hESCs to alternative fates, such as early endocardium specification, which then provides coordinating cues to the developing cardiac tissue via lateral inhibition.[41] Alternatively, microwell culture may encourage differentiation down multiple lineages or promote the activation of juxtacrine signaling due to increased cell–cell contact. However, the heterogeneity of EB-based differentiation makes studying which signaling pathways are most important in directing any specific cell fate difficult. Batch-to-batch variability exists among experiments and the composition of individual EBs within any single experiment is variable. The population-level overview of gene expression presented here highlights the fact that there are substantial differences in the signaling and differentiation trajectories between EBs made from hESCs cultured in 3-D microwells and on 2-D TCPS. The clearest difference was that genes associated with primitive streak, mesendoderm, and cardiac differentiation were upregulated in microwell-cultured hESCs and the resulting EBs.

These differences between EBs generated from 2-D substrates and 3-D microwells were likely influenced by the effects of 3-D culture and also the tighter control over EB size distribution that microwells confer. A previous study demonstrated that that the distribution of EB diameters generated from microwells could be described by Gaussian distributions tightly centered at the dimensions of the microwell confinement.[18] In contrast, as hESC colony size was not constrained in 2-D culture, EBs derived from hESCs cultured on 2-D substrates were more broadly size distributed and not well described by a simple Gaussian distribution. Studies utilizing both mouse and human ESCs that were aggregated into EBs within different-sized microwells have also indicated that EBs formed from microwell culture can affect lineage progression. Park et al.[42] reported higher expression of ectoderm-associated genes and proteins in EBs made in smaller microwells (100 μm), whereas the EBs from larger microwells favored mesoderm and endoderm gene expression (500 μm). Nguyen et al.[43] observed that EBs made from microwells around 100 μm preferentially upregulated endoderm and ectoderm markers when compared to EBs from smaller microwells. Bauwens et al.[44] controlled EB size by changing hESC colony size in 2-D using circular ECM islands of varying diameters. Their results indicated that aggregate size alone can play an important role in differentiation trajectories. Our recent study and others have also demonstrated that controlling EB size by changing 3-D microwell confinement dimensions influences cardiac differentiation.[18,22] However, the entire influence of 3-D culture cannot be restricted to the effects of EB size distribution control. Mohr et al.[18] generated EBs from 3-D microwells of dimensions ranging from 100 to 500 μm, which spans the range of EB sizes generated from unconstrained 2-D culture. In terms of cardiomyocyte differentiation efficiency quantified via flow cytometry and PCR for cardiomyocyte markers and fraction of beating EBs for functioning cardiomyocytes, EBs generated from all microwell sizes outperformed those from 2-D culture. These data suggest that the size differences in EBs generated from 2-D substrates and 3-D microwell culture cannot entirely account for the observed differences in cell signaling and differentiation fates.

In addition to observing substantial differences in gene expression during EB differentiation, we detected multiple molecular differences in undifferentiated hESCs cultured in 3-D and 2-D platforms. Culturing hESCs in a 3-D microenvironment increased functional cell–cell contact and modulated developmental signaling pathways including TGFβ/Activin/Nodal and BMP signaling, and Wnt/β-catenin signaling. We observed that hESCs cultured in microwells, as compared to 2-D, exhibited a lower ratio of phosphorylated Smad2 and a higher ratio of phosphorylated Smad1/5. This suggests less Smad signal transduction through the TGFβ/Activin/Nodal branch and more through the BMP branch. In hESCs, TGFβ/Activin/Nodal regulates pluripotency, whereas BMP signaling induces differentiation.[45,46] While this may suggest that hESCs cultured in microwells may be more primed for differentiation than those on 2-D, the percentage of Oct4 positive cells remained the same, as indicated in Figure 3B. Importantly, the BMP antagonist *NOGGIN* was more highly expressed in microwell-cultured hESCs. Noggin cooperates with Fgf2 to maintain pluripotency by inhibiting BMP signaling in hESCs.[47] In addition, we demonstrated that the amount of E-cadherin per cell was significantly higher in hESCs from microwells than from 2-D. This trend was further expounded upon in a study by Azarin et al.,[20] which demonstrated that the E-cadherin surface density was 5-fold higher in cells cultured in microwells. Moreover, Azarin et al. demonstrated that changing the dimensions of the 3-D microwells can modulate E-cadherin expression, further suggesting a link between the 3-D culture conditions and molecular changes like cell–cell contact. In a separate study, Nakazawa et al.[48] also linked the expression level of E-cadherin in mouse ESCs to microwell dimension. E-cadherin has been shown to function as both a regulator of pluripotent signaling pathways as well as improve hESC derivation.[49,50] Thus, the changes in other major signaling pathways, such as TGFβ/BMP and Wnt, may at least in part result from the increased cell–cell contact in the 3-D microwell culture to change the hESC cellular context. This may serve as a means to bias the cells toward the mesendoderm lineages during differentiation. Nonetheless, it is intriguing that by simply culturing hESCs in a 3-D microenvironment without additional changes to media or ECM, multiple pathways can be affected.

Furthermore, it is still unclear by what specific mechanisms these differences arise. The 3-D microenvironment can influence not only cell–cell contact but also cell-ECM contact, mechanical interactions between cells, cytoskeletal tension, and cell morphology. Due to the many changes a cell can experience when cultured in 3-D, it is reasonable that multiple mechanisms synergize to produce the range of molecular and signaling differences observed. However, it is also possible that one primary pathway is responsible for regulating the molecular differences observed during 3-D culture and directly activates other pathways.

The collective data from this study illustrate that 2-D and 3-D culture of hESC leads to distinct developmental signaling early in differentiation and may potentially provide molecular targets for studying pathways by which the 3-D microenvironment tranduces signals that prime hESCs for differentiation and influence desired differentiation outcomes. Not only may these molecular targets be exploited to engineer cell fate decisions in 2-D differentiation processes but also understanding how microenvironmental contributions from the intercellular and autoregulatory signaling that occur in 3-D culture of hESCs and their derivatives can aid in the transition to 3-D downstream applications, such as tissue engineering and regenerative medicine.

Acknowledgments

This work was supported by NIH grant R01 EB007534 and NSF grant EFRI 0735903. The authors would like to thank Amritava Das in assistance with Matlab and the WiCell Research Institute for providing cells and reagents. They also thank Prof. Bird for his inspiration and wish him a happy 90th birthday.

Literature Cited

1. Thomson JA, Itskovitz-Eldor J, Shapiro SS, Waknitz MA, Swiergiel JJ, Marshall VS, Jones JM. Embryonic stem cell lines derived from human blastocysts. *Science*. 1998;282(5391):1145–1147.
2. Odorico JS, Kaufman DS, Thomson JA. Multilineage differentiation from human embryonic stem cell lines. *Stem Cells*. 2001;19(3):193–204.
3. Greenow K, Clarke AR. Controlling the stem cell compartment and regeneration in vivo: the role of pluripotency pathways. *Physiol Rev*. 2012;92(1):75–99.
4. Pampaloni F, Reynaud EG, Stelzer EHK. The third dimension bridges the gap between cell culture and live tissue. *Nat Rev Mol Cell Biol*. 2007;8(10):839–845.
5. Kraehenbuehl TP, Langer R, Ferreira LS. Three-dimensional biomaterials for the study of human pluripotent stem cells. *Nat Methods*. 2011;8(9):731–736.
6. Burdick JA, Vunjak-Novakovic G. Engineered microenvironments for controlled stem cell differentiation. *Tissue Eng Part A*. 2009;15(2):205–219.
7. Bratt-Leal AM, Carpenedo RL, McDevitt TC. Engineering the embryoid body microenvironment to direct embryonic stem cell differentiation. *Biotechnol Prog*. 2009;25(1):43–51.
8. Keung AJ, Kumar S, Schaffer DV. Presentation counts: microenvironmental regulation of stem cells by biophysical and material cues. *Annu Rev Cell Dev Biol*. 2010;26:533–556.
9. Keung AJ, Healy KE, Kumar S, Schaffer DV. Biophysics and dynamics of natural and engineered stem cell microenvironments. *Wiley Interdiscip Rev Syst Biol Med*. 2010;2(1):49–64.
10. Peerani R, Zandstra PW. Enabling stem cell therapies through synthetic stem cell-niche engineering. *J Clin Invest*. 2010;120(1):60–70.
11. Hsiao C, Palecek SP. Microwell regulation of pluripotent stem cell self-renewal and differentiation. *Bionanoscience*. 2012;2(4):266–276.
12. Khademhosseini A, Ferreira L, Blumling J, Yeh J, Karp JM, Fukuda J, Langer R. Co-culture of human embryonic stem cells with murine embryonic fibroblasts on microwell-patterned substrates. *Biomaterials*. 2006;27(36):5968–5977.
13. Mohr JC, de Pablo JJ, Palecek SP. 3-D microwell culture of human embryonic stem cells. *Biomaterials*. 2006;27(36):6032–6042.
14. Sakai Y, Yoshida S, Yoshiura Y, Mori R, Tamura T, Yahiro K, Mori H, Kanemura Y, Yamasaki M, Nakazawa K. Effect of microwell chip structure on cell microsphere production of various animal cells. *J Biosci Bioeng*. 2010;110(2):223–229.
15. Hong S-H, Werbowetski-Ogilvie T, Ramos-Mejia V, Lee JB, Bhatia M. Multiparameter comparisons of embryoid body differentiation toward human stem cell applications. *Stem Cell Res*. 2010;5(2):120–130.
16. Ng ES, Davis RP, Azzola L, Stanley EG, Elefanty AG. Forced aggregation of defined numbers of human embryonic stem cells into embryoid bodies fosters robust, reproducible hematopoietic differentiation. *Blood*. 2005;106(5):1601–1603.
17. Burridge PW, Anderson D, Priddle H, Barbadillo Muñoz MD, Chamberlain S, Allegrucci C, Young LE, Denning C. Improved human embryonic stem cell embryoid body homogeneity and cardiomyocyte differentiation from a novel V-96 plate aggregation system highlights interline variability. *Stem Cells*. 2007;25(4):929–938.
18. Mohr JC, Zhang J, Azarin SM, Soerens AG, de Pablo JJ, Thomson JA, Lyons GE, Palecek SP, Kamp TJ. The microwell control of embryoid body size in order to regulate cardiac differentiation of human embryonic stem cells. *Biomaterials*. 2010;31(7):1885–1893.
19. Burridge PW, Thompson S, Millrod MA, Weinberg S, Yuan X, Peters A, Mahairaki V, Koliatsos VE, Tung L, Zambidis ET. A universal system for highly efficient cardiac differentiation of human induced pluripotent stem cells that eliminates interline variability. *PLoS One*. 2011;6(4):e18293.
20. Azarin SM, Lian X, Larson EA, Popelka HM, de Pablo JJ, Palecek SP. Modulation of Wnt/β-catenin signaling in human embryonic stem cells using a 3-D microwell array. *Biomaterials*. 2012;33(7):2041–2049.
21. Hwang Y-S, Chung BG, Ortmann D, Hattori N, Moeller H-C, Khademhosseini A. Microwell-mediated control of embryoid body size regulates embryonic stem cell fate via differential expression of WNT5a and WNT11. *Proc Natl Acad Sci USA*. 2009;106(40):16978–16983.
22. Bauwens CL, Song H, Thavandiran N, Ungrin M, Massé S, Nanthakumar K, Seguin C, Zandstra PW. Geometric control of cardiomyogenic induction in human pluripotent stem cells. *Tissue Eng Part A*. 2011;17(15–16):1901–1909.
23. Kimelman D, Griffin KJ. Mesoderm induction: a postmodern view. *Cell*. 1998;94(4):419–421.
24. Tada S, Era T, Furusawa C, Sakurai H, Nishikawa S, Kinoshita M, Nakao K, Chiba T, Nishikawa S-I. Characterization of mesendoderm: a diverging point of the definitive endoderm and mesoderm in embryonic stem cell differentiation culture. *Development*. 2005;132(19):4363–4374.
25. Pereira LA, Wong MS, Mei Lim S, Stanley EG, Elefanty AG. The mix family of homeobox genes–key regulators of mesendoderm formation during vertebrate development. *Dev Biol*. 2012;367(2):163–177.
26. Heldin C-H, Landström M, Moustakas A. Mechanism of TGF-beta signaling to growth arrest, apoptosis, and epithelial-mesenchymal transition. *Curr Opin Cell Biol*. 2009;21(2):166–176.
27. Liu Y, Asakura M, Inoue H, Nakamura T, Sano M, Niu Z, Chen M, Schwartz RJ, Schneider MD. Sox17 is essential for the specification of cardiac mesoderm in embryonic stem cells. *Proc Natl Acad Sci USA*. 2007;104(10):3859–3864.
28. Arnold SJ, Stappert J, Bauer A, Kispert A, Herrmann BG, Kemler R. Brachyury is a target gene of the Wnt/beta-catenin signaling pathway. *Mech Dev*. 2000;91(1–2):249–258.
29. Lian X, Hsiao C, Wilson G, Zhu K, Hazeltine LB, Azarin SM, Raval KK, Zhang J, Kamp TJ, Palecek SP. Robust cardiomyocyte differentiation from human pluripotent stem cells via temporal modulation of canonical Wnt signaling. *Proc Natl Acad Sci USA*. 2012;109(27):E1848–E1857.
30. Lian X, Zhang J, Azarin SM, Zhu K, Hazeltine LB, Bao X, Hsiao C, Kamp TJ, Palecek SP. Directed cardiomyocyte differentiation from human pluripotent stem cells by modulating Wnt/β-catenin signaling under fully defined conditions. *Nat Protoc*. 2013;8(1):162–175.
31. Laflamme MA, Chen KY, Naumova AV, Muskheli V, Fugate JA, Dupras SK, Reinecke H, Xu C, Hassanipour M, Police S, O'Sullivan C, Collins L, Chen Y, Minami E, Gill EA, Ueno S, Yuan C, Gold J, Murry CE. Cardiomyocytes derived from human embryonic stem cells in pro-survival factors enhance function of infarcted rat hearts. *Nat Biotechnol*. 2007;25(9):1015–1024.
32. Yang L, Soonpaa MH, Adler ED, Roepke TK, Kattman SJ, Kennedy M, Henckaerts E, Bonham K, Abbott GW, Linden RM, Field LJ, Keller GM. Human cardiovascular progenitor cells develop from a KDR+ embryonic-stem-cell-derived population. *Nature*. 2008;453(7194):524–528.
33. Kattman SJ, Witty AD, Gagliardi M, Dubois NC, Niapour M, Hotta A, Ellis J, Keller G. Stage-specific optimization of activin/nodal and BMP signaling promotes cardiac differentiation of mouse and human pluripotent stem cell lines. *Cell Stem Cell*. 2011;8(2):228–240.
34. Zhang J, Klos M, Wilson GF, Herman AM, Lian X, Raval KK, Barron MR, Hou L, Soerens AG, Yu J, Palecek SP, Lyons GE, Thomson JA, Herron TJ, Jalife J, Kamp TJ. Extracellular matrix promotes highly efficient cardiac differentiation of human pluripotent stem cells: the matrix sandwich method. *Circ Res*. 2012;111(9):1125–1136.
35. Beyer TA, Narimatsu M, Weiss A, David L, Wrana JL. The TGFβ superfamily in stem cell biology and early mammalian embryonic development. *Biochim Biophys Acta*. 2013;1830(2):2268–2279.
36. Lough J, Barron M, Brogley M, Sugi Y, Bolender DL, Zhu X. Combined BMP-2 and FGF-4, but neither factor alone, induces cardiogenesis in non-precardiac embryonic mesoderm. *Dev Biol*. 1996;178(1):198–202.
37. Böttcher RT, Niehrs C. Fibroblast growth factor signaling during early vertebrate development. *Endocr Rev*. 2005;26(1):63–77.
38. Lowell S, Benchoua A, Heavey B, Smith AG. Notch promotes neural lineage entry by pluripotent embryonic stem cells. *PLoS Biol*. 2006;4(5):e121.

39. Nemir M, Croquelois A, Pedrazzini T, Radtke F. Induction of cardiogenesis in embryonic stem cells via downregulation of Notch1 signaling. *Circ Res*. 2006;98(12):1471–1478.
40. Niessen K, Karsan A. Notch signaling in cardiac development. *Circ Res*. 2008;102(10):1169–1181.
41. de la Pompa JL, Epstein JA. Coordinating tissue interactions: notch signaling in cardiac development and disease. *Dev Cell*. 2012;22(2): 244–254.
42. Park J, Cho CH, Parashurama N, Li Y, Berthiaume F, Toner M, Tilles AW, Yarmush ML. Microfabrication-based modulation of embryonic stem cell differentiation. *Lab Chip*. 2007;7(8): 1018–1028.
43. Nguyen D, Sa S, Pegan JD, Rich B, Xiang G, McCloskey KE, Manilay JO, Khine M. Tunable shrink-induced honeycomb microwell arrays for uniform embryoid bodies. *Lab Chip*. 2009;9(23): 3338–3344.
44. Bauwens CL, Peerani R, Niebruegge S, Woodhouse KA, Kumacheva E, Husain M, Zandstra PW. Control of human embryonic stem cell colony and aggregate size heterogeneity influences differentiation trajectories. *Stem Cells*. 2008;26(9):2300–2310.
45. Dalton S. Signaling networks in human pluripotent stem cells. *Curr Opin Cell Biol*. 2013;25(2):241–246.
46. Li W, Ding S. Human pluripotent stem cells: decoding the naïve state. *Sci Transl Med*. 2011;3(76):76ps10.
47. Wang G, Zhang H, Zhao Y, Li J, Cai J, Wang P, Meng S, Feng J, Miao C, Ding M, Li D, Deng H. Noggin and bFGF cooperate to maintain the pluripotency of human embryonic stem cells in the absence of feeder layers. *Biochem Biophys Res Commun*. 2005; 330(3):934–942.
48. Nakazawa K, Yoshiura Y, Koga H, Sakai Y. Characterization of mouse embryoid bodies cultured on microwell chips with different well sizes. *J Biosci Bioeng*. 2013;116(5):628–633.
49. Soncin F, Ward CM. The function of E-cadherin in stem cell pluripotency and self-renewal. *Genes (Basel)*. 2011;2(1):229–259.
50. Redmer T, Diecke S, Grigoryan T, Quiroga-Negreira A, Birchmeier W, Besser D. E-cadherin is crucial for embryonic stem cell pluripotency and can replace OCT4 during somatic cell reprogramming. *EMBO Rep*. 2011;12(7):720–726.

Manuscript received Oct. 3, 2013, and revision received Dec. 19, 2013.